Electronic Supplementary Information

Organic semiconductor polymers: A carbazole-based novel tribopositive polymer for energy harvesting with high temperature stability

Rayyan Ali Shaukat [a†], Shahid Ameen [b, c†], Qazi Muhammad Saqib [a], Mahesh Y. Chougale [a], Jungmin Kim [a], Swapnil R. Patil [a], Muhammad Noman [a], Hwan Kyu Kim[b], and Jinho Bae [a*]

[a] Department of Ocean System Engineering, Jeju National University, 102 Jejudaehakro, Jeju 63243, Republic of Korea

[b] Global GET-Future Lab and Department of Advanced Materials Chemistry, Korea University, 2511 Sejong-ro, Sejong 339-700, Korea.

[c] Department of Chemistry, Kohat University of Science and Technology (KUST), Kohat 26000, Pakistan.

*E-mail: baejh@jejunu.ac.kr

† Both authors are considered as the first contributing authors of this manuscript

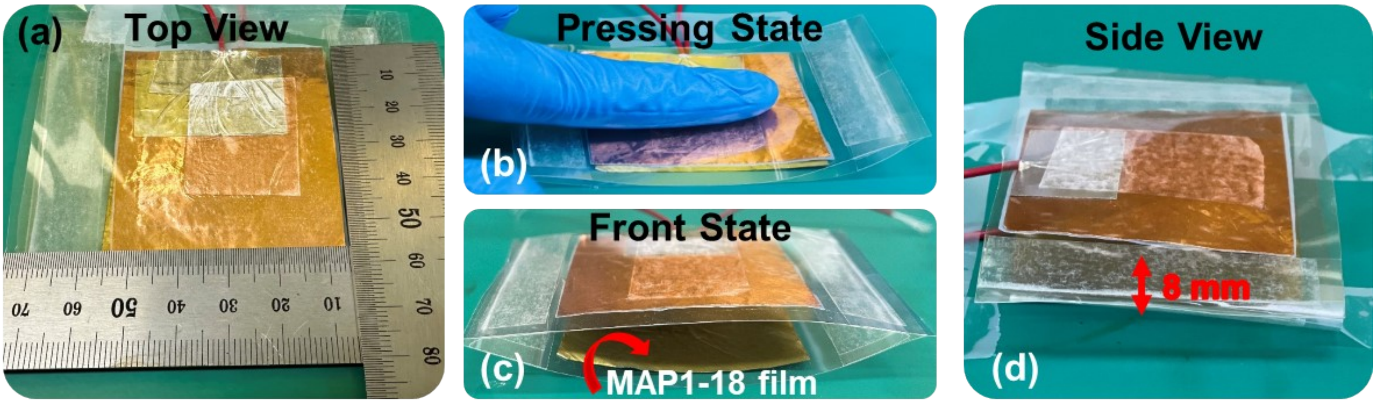

Fig. S1. Photographs of the fabricated MAP1-18/PTFE based TENG. a) Top view of the device along with the device area, b) pressing state of the device, (c) front view showing MAP1-18 film, and (d) side view of the device presenting the separation distance.

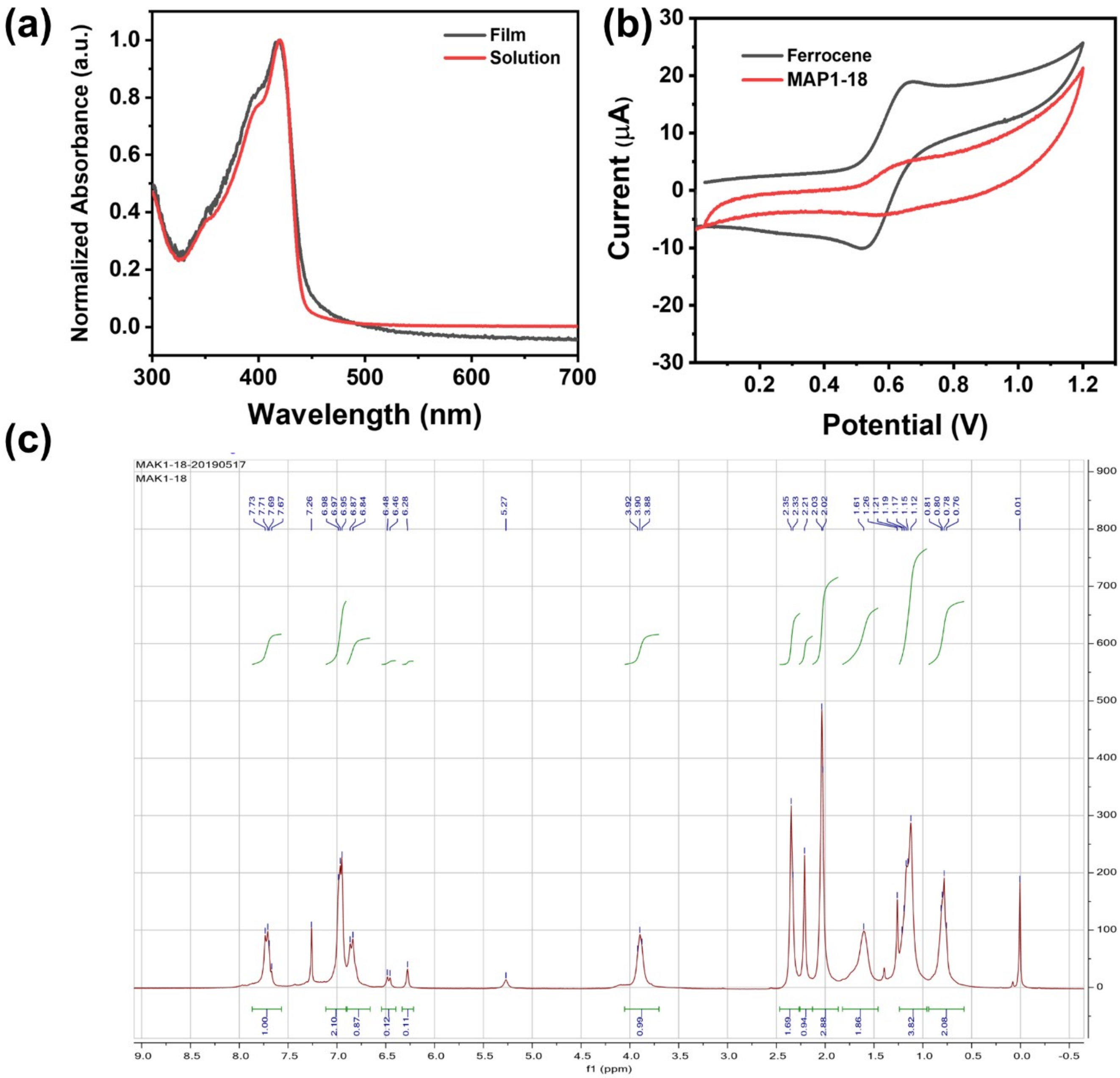

Fig. S2. (a) UV−Vis absorption spectra of MAP1-18 as a solution in dichloromethane (DCM) and as a thin film, (b) cyclic voltammogram of MAP1-18 solution in dichloromethane, and (c) H-NMR spectrum of MAP1-18.

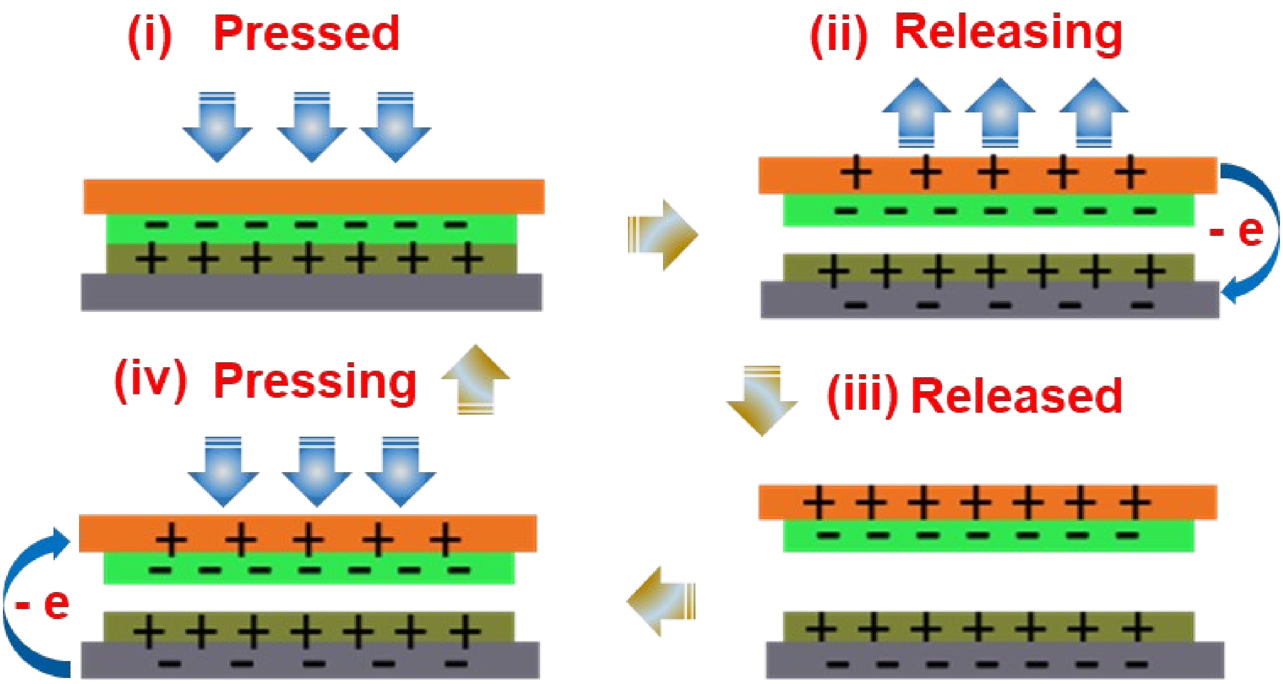

Fig. S3. Operating working mechanism of the proposed MAP1-18/PTFE based TENG device.

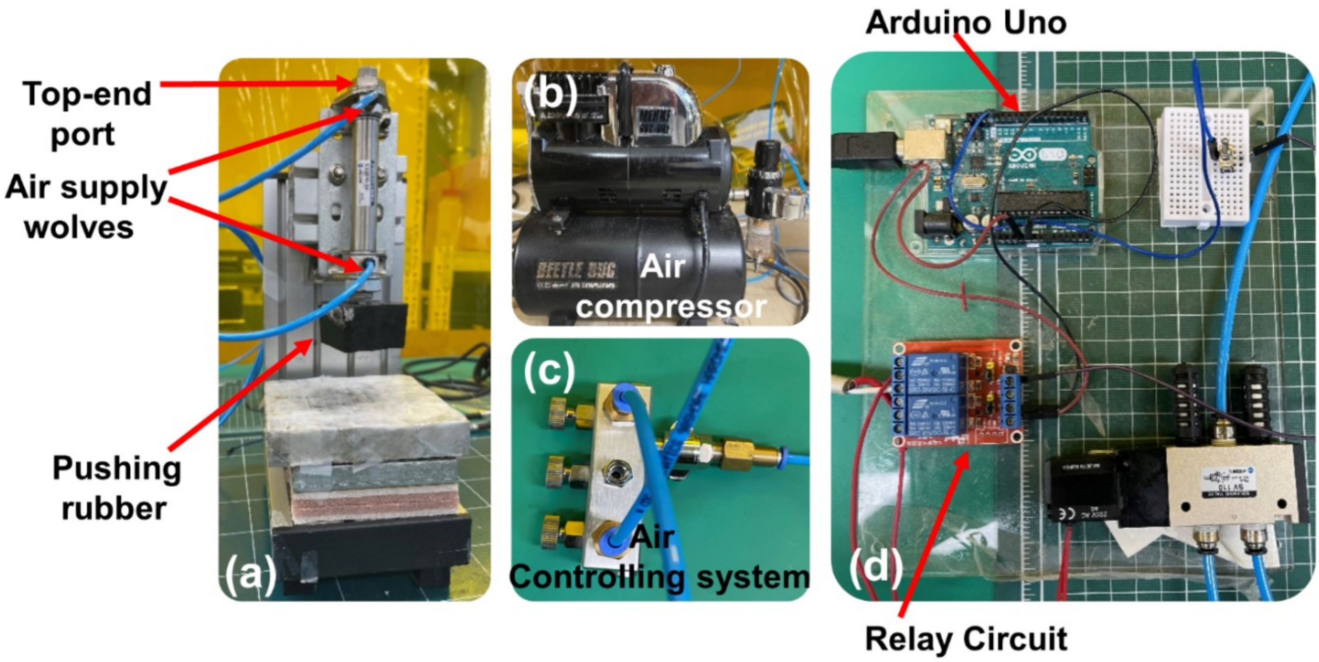

Fig. S4. Experimental setup used for the electrical characterization of the MAP1-18/TENG device. (a) Vertically aligned homemade pneumatic air cylinder, (b) photograph of the air compressor, (c) photograph of the air controlling system, and (d) realized image of the air controlling circuit.

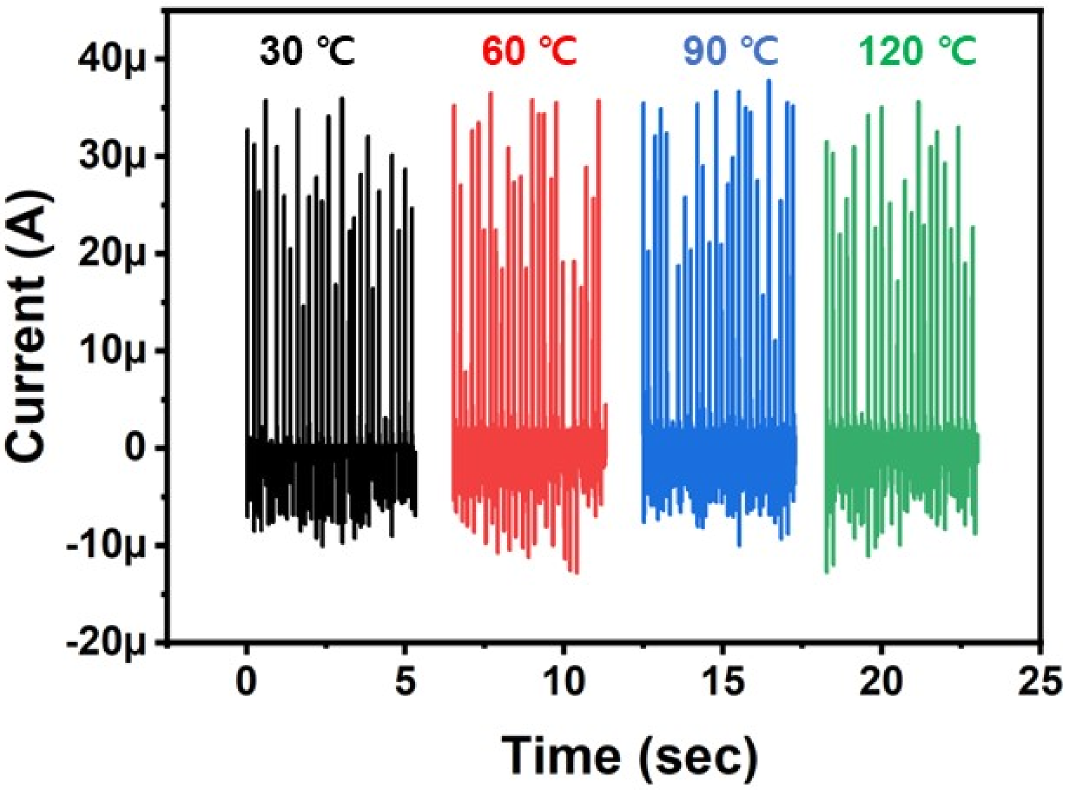

Fig. S5. Temperature dependent current curves of MAP1-18/TENG device from 30 ℃ to 120 ℃.

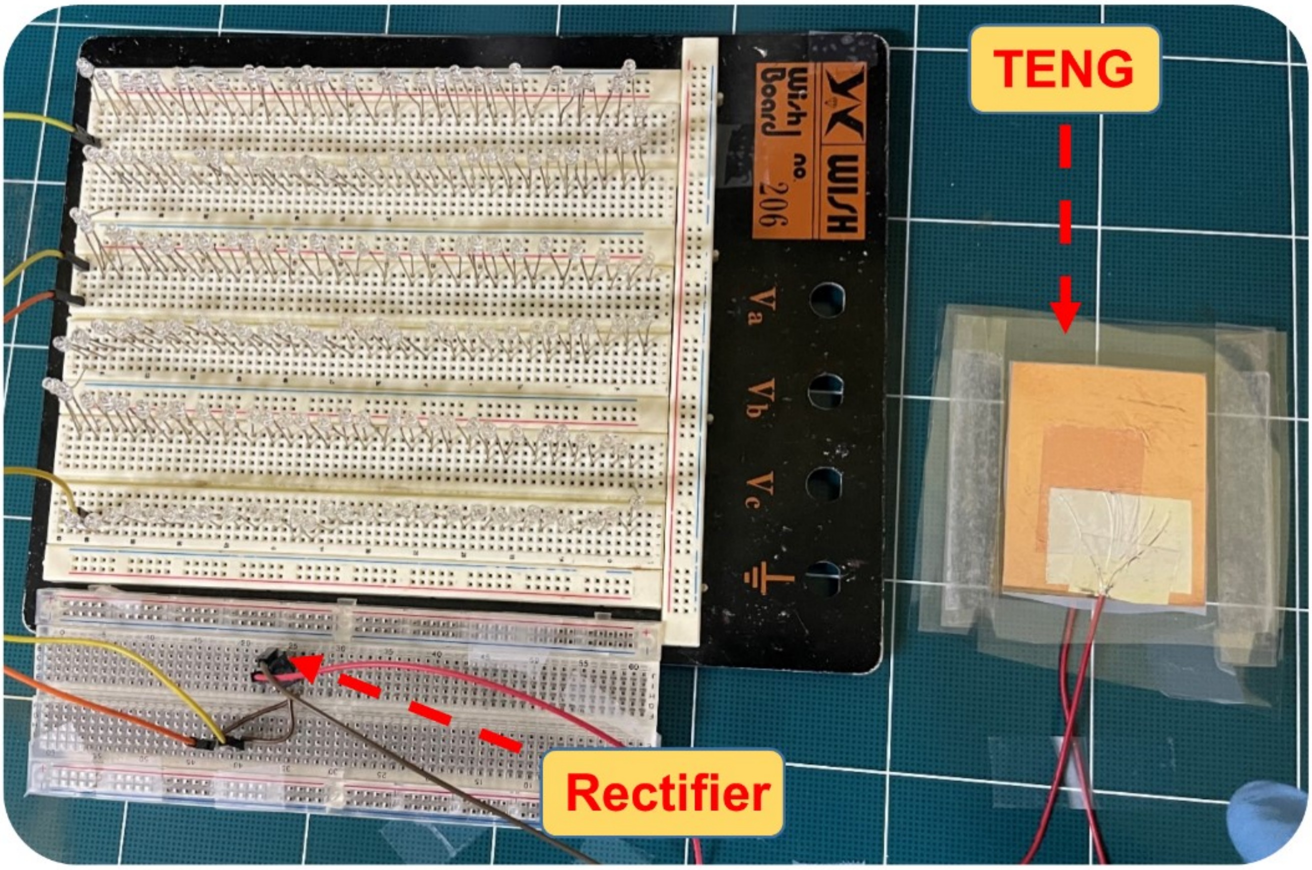

Fig. S6. Photograph of the light emitting diodes (LEDs) driven by the MAP1-18/PTFE based TENG device. The detailed operation of this setup can be seen in Supplementary Movie S1.

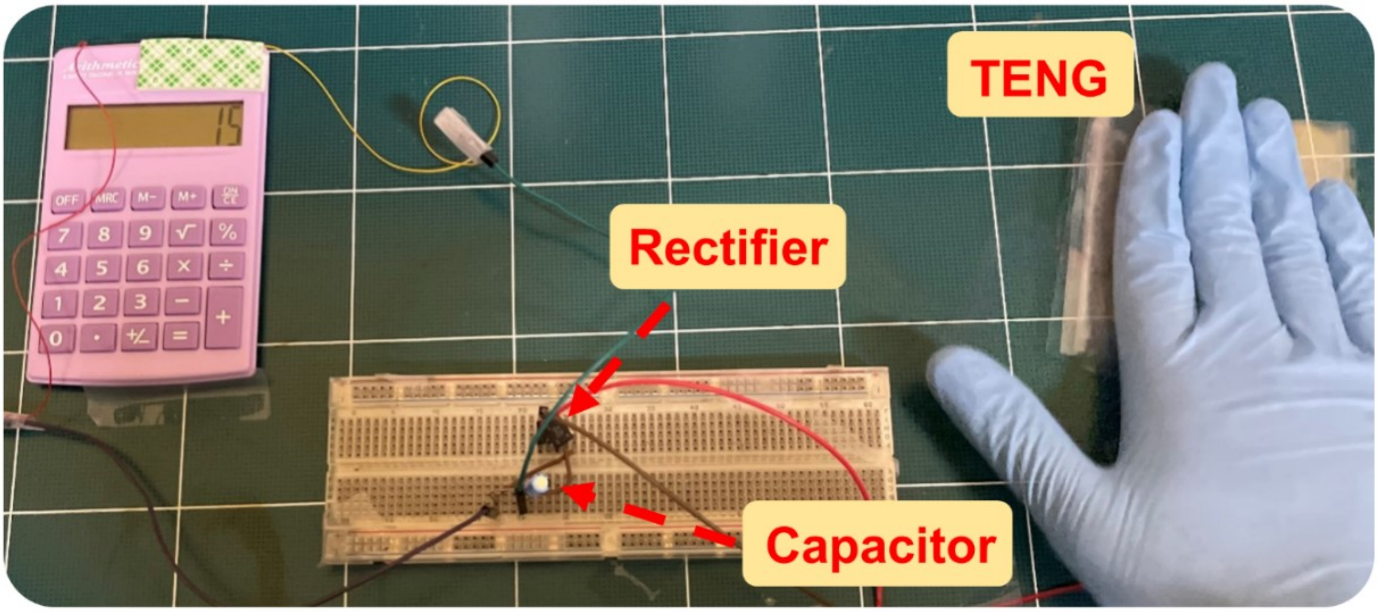

Fig. S7. Photograph of the circuit diagram of the powering the calculator with MAP1-18/PTFE based TENG device. The detailed operation of this setup can be seen in Supplementary Movie S2.

Note S1: The energy conversion efficiency of Carbazole triphenylamine (MAP1-18) based TENG

The energy conversion efficiency *(η)* is defined as the ratio of output electrical to input kinetic energy. In this case, the kinetic energy (KE) applied to the TENG device can be considered as the input energy while the electrical energy generated by the TENG device serves as the output energy. The input kinetic energy is defined as

$$E_k = \frac{1}{2} m v^2 \tag{1}$$

Here, the load mass is denoted by m, while its moving velocity is indicated by v. In the temperature range of -10 to 70 °C, the pneumatic air cylinder can be operated by applying air pressure ranging from 0.51 kgf / cm^2 (0.05 MPa) to 7.65 kgf / cm^2 (0.75 MPa). The piston rod's diameter is 6 mm, while the internal diameter of the cylinder is 16 mm. When the minimum air pressing is 0.51 kgf / cm^2, the out-stroke and in-stroke driving forces are 1.025 kgf and 0.4 kgf, respectively. The square rubber (load mass) of 48 g is installed on the top rod of the cylinder to press the proposed device, as shown in Fig. S4a. The average mass of a squared rubber fixed on the top rod of the cylinder was calculated to be 0.048 kg. When mass (m) is 0.048 kg, velocity (v) is 0.26 m/s. The velocity (v) can be calculated as v = x/t, where x = 2.6 cm is down and up moving distance of the load mass and t is 0.1 s. So, kinetic energy (KE) can be calculated as 1.62 mJ. The output electrical energy ($E_{electrical}$) of MAPI-18 based TENG was measured on the load resistance of 20 MΩ, respectively. From the measured results, the $E_{electrical}$ can be calculated as bellows:

$$E_{electrical} = \int_0^t I^2 R dt = \int_0^t \frac{V^2}{R} dt \tag{2}$$

Here, I is measured current, R is load resistance, and t is measuring time. It can be observed that the values of output electric energy from MAPI-18 based TENG, were obtained as 0.0002281 J. The TENG device energy conversion efficiency (*η*) was calculated as

$$\textit{Energy Conversion Efficiency } (\eta) = \frac{output\ electric\ energy}{input\ kinetic\ energy} \times 100\ [\%] \tag{3}$$

Consequently, the *η* of the proposed MAPI-18 based TENG devices were reached to ~14.06%.

Table S1. Comparison of the electrical performances of the previously reported OSP's nanogenerators with our proposed MAP1-18/PTFE based TENG device. The output performance of the TENG depends upon the electron accepting or donating ability of the triboelectric materials. The organic semiconducting polymer MAP1-18 carries strong electron donating ability compared with previously reported polymers. Hence, large improvements were observed in the output performance of the fabricated TENG device. Table S1 presented the TENG devices based on various polymers like PEDOTT: PSS and polypyrrole (PPy). These polymers have conducting nature and carries moderate electron donating or accepting capability, thus showing less device performance compared to MAP1-18 based TENG device.

Device Structure	Device Mechanism	Force (N)	Frequency (Hz)	Voltage (V)	Current (μA)	Power	Ref.
Al/polypyrrole (PPy)/Au	Schottkey Dc generator	---	---	0.73	---	0.21 W/m^2	1
$Au/PPy/SnO_2/Al$	Dc Energy Generator	---	---	0.2	3.6	---	2
Al/PEDOTT: PSS/ Ni	Tribovoltic effect	0.15	1.25	0.7	2	1.1 mW/m^2	3
Al/carbazole triphenylamine/ PTFE/Cu	**Vertical contact-separation**	**58**	**10**	**796 V**	**46**	**148 $\mu W/cm^2$**	**Our work**

References

1. H. Shao, J. Fang, H. Wang, H. Niu, H. Zhou, Y. Cao, F. Chen, S. Fu and T. Lin, *Nano Energy*, 2019, **62**, 171-180.
2. H. Shao, J. Fang, H. Wang, H. Zhou and T. Lin, *Journal of materials chemistry A*, 2017, **5**, 8267-8273.
3. J. Meng, Z. H. Guo, C. Pan, L. Wang, C. Chang, L. Li, X. Pu and Z. L. Wang, *ACS Energy Letters*, 2021, **6**, 2442-2450.